Detection of physiological changes after exercise via a remote opto-physiological imaging system

Yu Sun[1,2], Sijung Hu[1*], Vicente Azorin-Peris, Jia Zheng[1], Stephen Greenwald[3], Jonathon Chambers[1], Yisheng Zhu[2]

[1] Department of Electronic and Electrical Engineering, Loughborough University, Ashby Road, Loughborough, Leicestershire, LE11 3TU, UK

[2] Department of Biomedical Engineering, Shanghai Jiao Tong University, 800 Dongchuan Road, Shanghai, 200240, P. R. China

[3] Pathology Group, Institute of Cell & Molecular Science, Barts & The London School of Medicine and Dentistry, London, E1 2ES, UK

ABSTRACT

A study of blood perfusion mapping was performed with a remote opto-physiological imaging (OPI) system coupling a sensitive CMOS camera and a custom-built resonant cavity light emitting diode (RCLED) ringlight. The setup is suitable for the remote assessment of blood perfusion in tissue over a wide range of anatomical locations. The purpose of this study is to evaluate the reliability and stability of the OPI system when measuring a cardiovascular variable of clinical interest, in this case, heart rate. To this end, the non-contact and contact photoplethysmographic (PPG) signals obtained from the OPI system and conventional PPG sensor were recorded simultaneously from each of 12 subjects before and after 5-min of cycling exercise. The time-frequency representation (TFR) method was used to visualize the time-dependent behavior of the signal frequency. The physiological parameters derived from the images captured by the OPI system exhibit comparable functional characteristics to those taken from conventional contact PPG pulse waveform measurements in both the time and frequency domains. Finally and more importantly, a previously developed opto-physiological model was employed to provide a 3-D representation of blood perfusion in human tissue which could provide a new insight into clinical assessment and diagnosis of circulatory pathology in various tissue segments.

Keywords: Photoplethysmography (PPG), Opto-physiological imaging (OPI), Time-frequency representation (TFR), Blood perfusion mapping, Physiological variables, Bland Altman plots, Pseudo-Wigner-Ville distribution (SPWVD)

1. INTRODUCTION

Assessments of the peripheral pulse with photoplethysmography (PPG) can provide information about the cardiovascular system, such as blood oxygen saturation, heart and respiration rates, cardiac output and blood pressure [1]. PPG, first described in the 1930s [2], is an optical biomonitoring technique that non-invasively measures arterial pulsations in-vivo and its ease of use and convenience make it an attractive area of research in the biomedical and clinical community. Although successful, conventional contact PPG is not suitable in situations of skin damage (burn/ulcer), or when free movement is required. One potential way to overcome these problems is to use the recently introduced technique of imaging PPG, a remote, contactless diagnostic technique that can assess peripheral blood perfusion [3-5].

Although numerous epidemiologic studies provide strong evidence that occupational or recreational exercise not only maintains fitness but also boosts the immune system and reduces mortality from cardiovascular disease [6], there is also evidence that excessive exercise is hazardous and may result in sudden death [7]. The "dose" of exercise, i.e. intensity, duration, and frequency of training required to achieve and optimize the beneficial response, however, have yet to be fully understood [8]. Hence, it is worthwhile to develop a remote technique capable of offering reliable assessment of the cardiovascular system during/after exercise. Recently, Wieringa and colleagues have introduced a multiple wavelength imaging PPG device that provides a possible route toward contactless blood oxygen saturation assessment [4], and Verkruysse has reported a digital camera based on a remote PPG signal acquisition technique, using ambient light illumination[5]. This has stimulated our interest in the remote assessment of the cardiovascular system to evaluate the influence of exercise through imaging PPG measurement. Furthermore, our group at Loughborough University have demonstrated an integration of imaging PPG setup for the detection of tissue opto-physiological properties[11].

In this paper, we show that PPG signals obtained after exercise can be remotely accessed by our opto-physiological imaging (OPI) system. To assess the influence of different exercise levels on the cardiovascular system, the nature of pulsatile variations in the PPG signal under different exercise levels was studied. The results of this study prove the

* S.Hu@lboro.ac.uk; phone: +44 1509 227058

Design and Quality for Biomedical Technologies IV, edited by Ramesh Raghavachari, Rongguang Liang,
Proc. of SPIE Vol. 7891, 78910E · © 2011 SPIE · CCC code: 1605-7422/11/$18 · doi: 10.1117/12.872723

practicability of the OPI system and also provide an insight into possible future clinical assessment using this technology.

2. MATERIALS & METHODS

2.1 Subjects

A total of twelve healthy subjects (male/female=10/2; age=31.3±12.7 yrs; height=1.77±0.07 m; BMI=23.5±3.5 kg m^{-2}) recruited from Loughborough University were enrolled in this study. Four of the participants are habitual smokers with over 6 years smoking history. None of the subjects had any known cardiovascular disease and none were diabetic. Informed consent was obtained from all of the subjects and approved by the university ethical committee in compliance with the Declaration of Helsinki. The subjects were asked to refrain from consuming caffeine or alcohol, and asked not to smoke or undertake strenuous exercise for the two hours preceding the study.

2.2 Opto-physiological system setup

The OPI system is schematically presented in Fig.1. A monochrome CMOS camera (Model: Eo*Sens* MC1360-63, Mikrotron, Germany) with maximum resolution of 1280×1024 pixels was focused on the palm of the participant's right hand using an industry-standard F-mount zoom lens (Model: Nikkor 20 mm f/2.8D, Nikon, Japan). The pixels were encoded in a 10 bit gray scale, allowing the camera to detect the weak pulsations of the microvascular tissue bed. A custom built infrared (λ=870 nm) ringlight illumination source (RIS) comprising 100-RCLEDs (Model: 0603SMD, JMSienna) fitted into a ring reflector, was mounted around the lens to collimate and homogenize the distribution of light. The RIS was current-controlled and synchronized with the camera capture cycle. The distance between camera lens/RIS and skin was approximately 350 mm. In all experiments, a commercial pulse oximeter contact sensor (Model: P871RA, Viamed, UK) was placed on the index finger of the right hand to measure the participant's pulse signal for validation. The analog signal outputs from the contact sensor were digitized using a DISCO4 (Dialog Devices, UK) data acquisition system incorporating a 12-bit A/D converter running at a sample rate of 128 Hz. The images captured from the camera were synchronized to the physiological signals acquired from the contact sensor via an additional signal from the camera to the A/D converter.

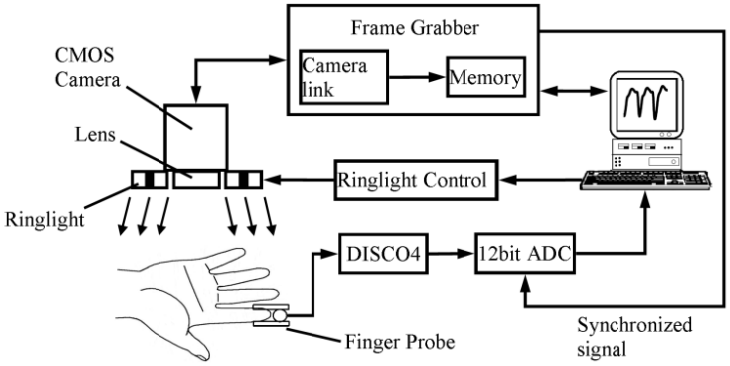

Figure1. Experimental setup of the non-contact OPI system.

2.3 Experimental protocol

The experimental procedures are depicted in Fig.2. All measurements were made in a temperature-controlled darkroom (27±1 °C) by a trained operator. Upon arrival, the subjects were required to sit on an adjustable chair and rest for at least 10 min before a blood pressure measurement were taken from the left arm using a clinically validated digital blood pressure monitor (Model: M6, Omron, Japan). Afterwards, participants were asked to sit at ease and rest their right hand as still as possible during the examination. The right palm of each participant was exposed to the infrared RIS and recorded with the CMOS camera. For each subject, images were recorded for 34 s at a rate of 50 fps and exposure time of 15 ms. The size of the raw image was 640×480 pixels. Contact PPG was recorded from the finger probe for about 3 minutes to verify that the heart rate was stable. Approximately 60 seconds later, the camera was started, at which time a synchronization signal was activated for simultaneous recording with the finger probe measurements. Then, the subject was asked to ride a cycling machine (Model: XR-580, PowerTrek, UK) at a speed of 15 km/h (*exercise 1*) for 5 minutes. Immediately after the exercise, participants' blood pressure and the second 34 s video was acquired. After 10 minutes

rest, another 5 minutes exercise was performed at 25 km/h (*exercise 2*) and the post-exercise data acquisition procedures were repeated. A final measurement was made after a further 10 minute rest period.

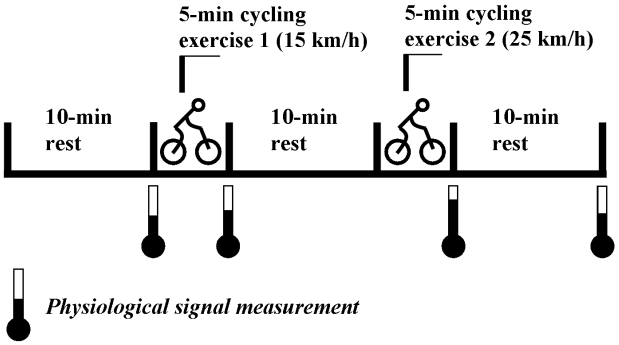

Figure 2. Schematic of the experimental protocol.

2.4 Image processing

After a set of recordings were acquired, the raw image frames were divided into discrete sub-windows and a new set of reduced frames were calculated, where the value of each pixel in the reduced frame was set as the average of all the pixel values within each sub-window. Though compromising the spatial resolution, such a procedure was found to significantly improve the signal to noise ratio [5]. For the mapping, the optimum window size was found to be 10×10 pixels. This resulted in a reduced frame size of 64×48 pixels, yielding PPG signals at each pixel position across a sequence of frames. The PPG signals were then band-pass filtered using a 5th order Butterworth filter. Cut-off frequencies were set at [0.5, 4] Hz to allow a wide range of heart rate measurements.

Prior studies have shown that light intensity in tissue can be described by the Beer-Lambert law [9]:

$$I_o = I_i \cdot exp\,(-\mu_{a,s}L_s) \cdot exp\,(-\mu_{a,a}L_a) \tag{1}$$

where I_o is the transmitted light intensity, I_i is the incident light intensity; $\mu_{a,s}$ is the wavelength-dependent absorption coefficient of the static component of tissue, in units of cm^{-1}; and $\mu_{a,a}$ is the absorption coefficient of the arterial blood; and L_s and L_a, represent, respectively, the optical path length of static and arterial components. The latter, pulsatile (ac) component, attributed to changes in blood volume synchronous with the heartbeat [10], can be expressed as:

$$\Delta I_o = -I_i\mu_{a,a} \cdot exp\,(-\mu_{a,s}L_s) \cdot exp\,(-\mu_{a,a}L_a) \cdot \Delta L_a \tag{2}$$

The PPG waveform comprises a pulsatile (ac) physiological waveform which is superimposed on a slowly varying (dc) baseline [1]. The ac/dc ratio is acquired through normalization: $\Delta I_o/I_o = -\mu_{a,a}\Delta L_a$, which depends upon the relative changes in the arterial optical path length ΔL_a.

We have previously presented a Monte Carlo (MC) simulation based opto-physiological model of multi-layered skin tissue [11]. With unique tissue optical properties and specified geometries, each layer contributes differently to the changes of arterial optical path length. In this study, a six-layer skin tissue model [12] was employed in a MC simulation to obtain the contribution of each layer to ΔL_a. The arterial pulsation was simulated by adding pulsatile blood into non-pulsatile tissue, consequently changing the volume fraction. Hence, the blood perfusion map of each specific layer could be calculated.

2.5 Signal processing

Fourier Transform (FT), which offers a passage from the time domain to the frequency domain, is widely utilized in conventional PPG signal processing as it straightforwardly provides fundamental information such as heart rate and respiration rate [4, 13]. However, it does not allow a combination of the two domains. Hence, it could lead to ambiguous results since it assumes that signals are steady-state when, in reality, physiological signals are generally transient in nature. Hulsbusch and colleagues have shown that the uncritical use of the FT could lead to misinterpretation of perfusion PPG signals [3]. Therefore, to obtain a potentially more revealing picture of the temporal localization of a signal's spectral components, one has to resort to the joint time-frequency analysis, e.g., time-frequency representation (TFR). The TFR approach converts a one-dimensional time signal into a two dimensional function of time and frequency

so that frequency components can be localized with a good temporal resolution [14]. In this study, a smoothed pseudo-Wigner-Ville distribution (SPWVD) was chosen for TFR estimation of the obtained PPG signals:

$$SPWVD(t,f) = \int h(\tau) \int g(s-t) x\left(s+\frac{\tau}{2}\right) x^*(s-\frac{\tau}{2}) e^{-j2\pi f\tau} ds d\tau \quad (3)$$

where $g(s)$ and $h(\tau)$ are two windows whose effective lengths independently determine the time and frequency smoothing spread respectively.

3. RESULTS

3.1 Physiological variables

As mentioned previously, four physiological measurements were performed, i.e., rest, post-ex1, post-ex2, and recovery. Fig.3 shows the measured variables: heart rate (HR), systolic blood pressure (SBP), and diastolic blood pressure (DBP).

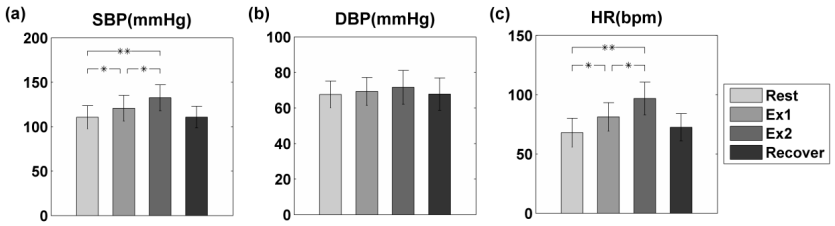

Figure.3 Effects of exercise on blood pressure and heart rate. Each bar represents the average SBP (a), DBP (b), and HR (c) for each state (rest, ex1, ex2, and recovery). Error bars show standard deviations. Significant statistical differences are indicated with * for $p<0.05$ and ** for $p<0.01$.

To demonstrate the influence of exercise on the cardiovascular system, ANOVA was conducted on each of the measured variables. Post hoc analysis with Duncan's test was also employed. The results are shown in Fig.3. ANOVA SBP and HR showed a significant influence of exercise (F=7.608, p=0.001 & F=12.666, p=0.000). Post hoc tests revealed that compared to the rest condition, the HR and SBP were significantly higher after both exercise levels (ex1 *vs.* rest, $p<0.05$, ex2 *vs.* rest, $p<0.01$). In addition, a significant difference between different exercise levels was also observed in HR and SBP. Specifically, higher HR (p=0.004) and SBP (p=0.039) were revealed aftert exercise 2 (25 km/h) compared to the moderate exercise level (15 km/h). After 10 mins rest, the hemodynamic parameters all returned to the rest level. No significant effect of exercise on DBP was observed.

3.2 Heart rate estimation (iPPG *vs.* cPPG)

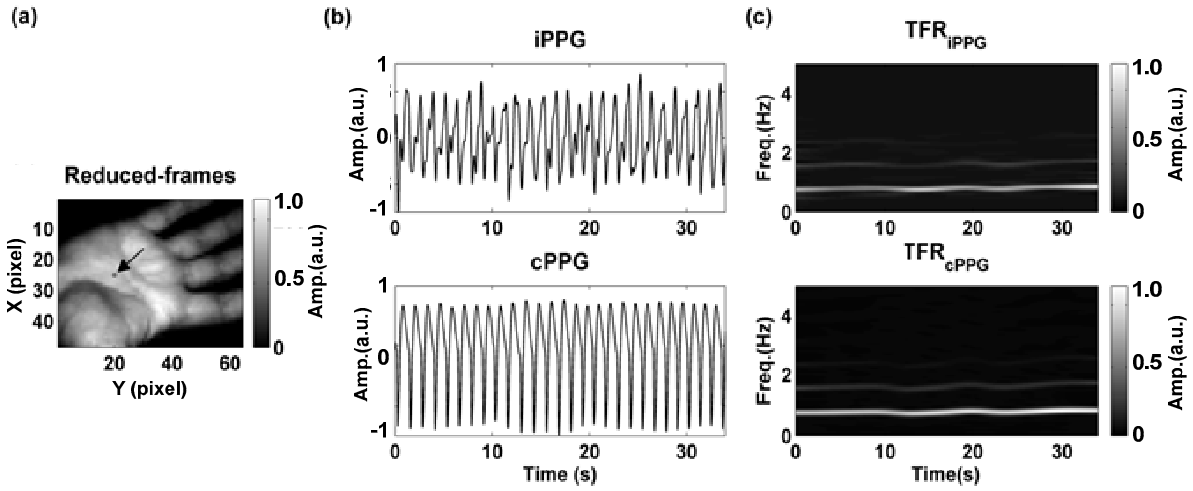

Figure 4. A representative figure showing a reduced frame with greyscale sidebar showing the signal amplitude (a), PPG signals (b), and the corresponding TFR results (c). The upper TFR trace is from the non contact imaging PPG and lower is from contact

PPG with the greyscale indicating the power intensity. The signal is from Subject #7 (Male, age=55 yrs) at rest condition. The position from which the iPPG signal was obtained is highlighted with a black box (x=20, y=25) and an arrow.

Fig. 4 is an example of the PPG signals obtained from a single subject and the TFR, in which the HR frequency and 2nd harmonic components are shown. Additionally, the HR derived from the TFR plot is found to be in excellent agreement with the HR obtained from the commercial pulse oximeter sensor readings. A slowly varying HR is also detected from the TFR trace which indicates the potential usage of TFR in revealing the time-varying HR during the exercise.

To evaluate the reliability and stability of the OPI system, Bland Altman plots were employed to compare the agreement between the imaging-PPG (iPPG) and contact-PPG (cPPG) measurements [15]. The HR_{iPPG} is obtained through averaging the HR within all the sub-windows (64×48 pixels). Historical estimations of the HR were used to define a threshold for maximum deviation in HR among different regions. The HR calculation was started in the middle of the processed frames (x=32, y=24), using the HR within this region as a reference. Successive calculations were then performed where, if the difference between the current HR estimation and the reference value exceeded the threshold (9 bpm in this study), the algorithm isolated it as a non-tissue or corrupt area and rejected the invalid HR.

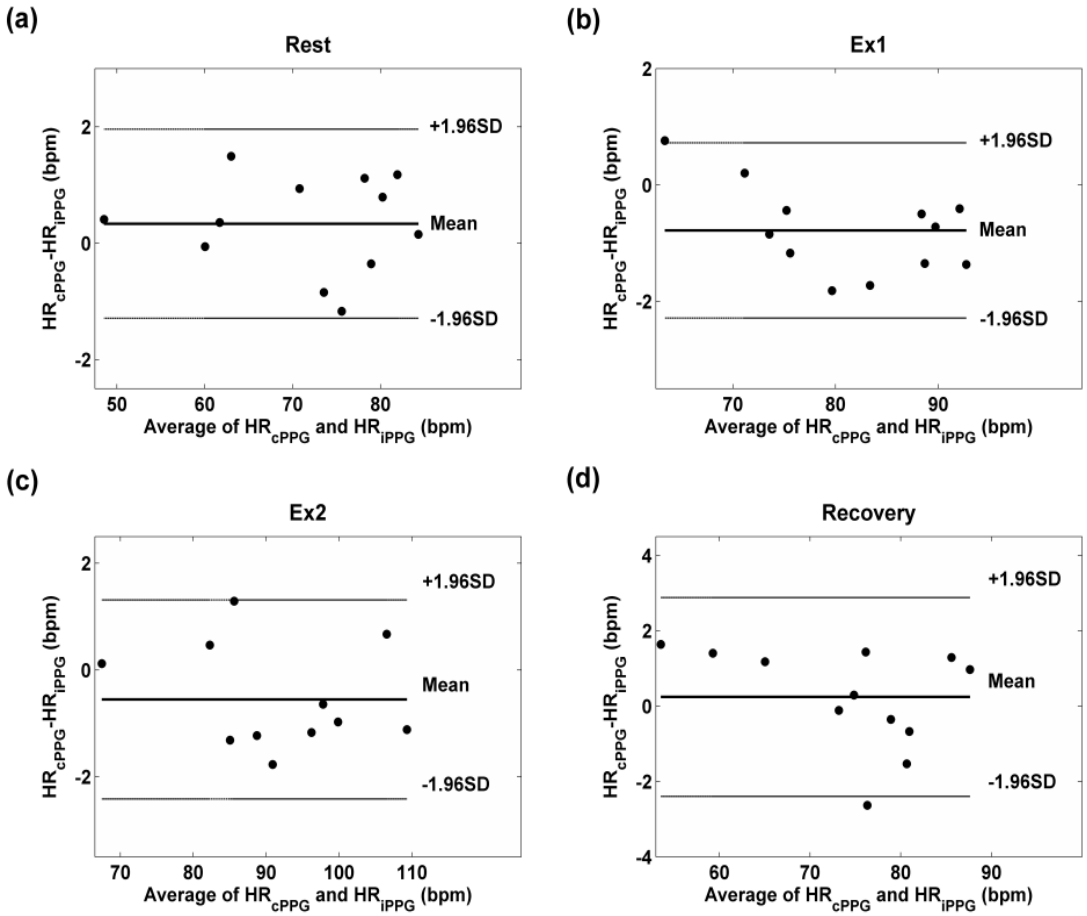

Figure 5. Bland Altman plots showing the average of the HR measured by the cPPG and iPPG, plotted against the difference between their measurements for each subject at (a) rest, (b) post-exercise 1, (c) post-exercise 2, and (d) recovery states.

Fig.5 shows a comparison of HR measured from cPPG and iPPG. Specifically, the mean bias is 0.33 bpm with 95% limits of agreement -1.29 to 1.96 bpm in the rest state. While the mean bias obtained after the first and second exercise periods are -0.78 and -0.55 bpm respectively. The corresponding 95% limits of agreement are from -2.29 to 0.73 bpm and -2.42 to 1.32 bpm. After 10 minutes rest, the mean bias is 0.24 bpm with 95% confidence interval -2.40 to 2.88 bpm. Moreover, significant correlation coefficients between both measurements are revealed in all states (Pearson's correlation, $r^2>0.9$, $p<0.01$).

3.3 Blood perfusion mapping

As mentioned in the *Image processing* section, a six-layer tissue model was employed in a Monte Carlo simulation to obtain the contribution of each layer to the output signals by accounting for the absorption (i.e., photon packet intensity) and scattering (i.e., optical path length) properties of tissue. The minima and maxima of the PPG signals were identified using a custom algorithm in Matlab. The amplitude of the PPG signal was then determined for each pulse and the mean peak-to-peak amplitude served as the *ac* part. The slowly varying baseline was obtained by low pass filtering the PPG signal (<0.5 Hz), and the mean value of the baseline was taken as the dc component. Accordingly, the ac/dc ratio for each ROI could be calculated. Fig.6 shows a layered blood perfusion map from a subject at rest.

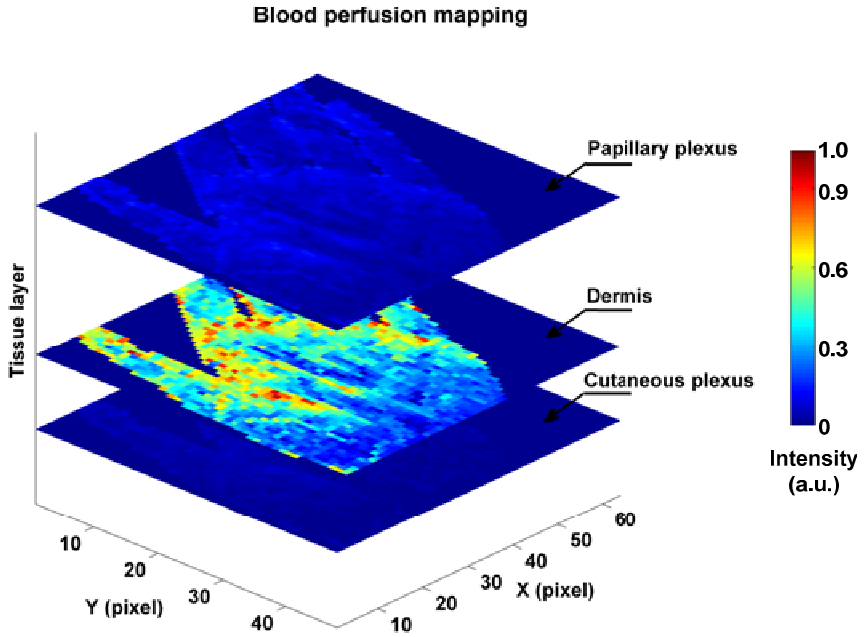

Figure 6. Layered blood perfusion map with color bar indicating the intensity (a.u.). The signal is from Sub#6 (Male, age: 27 yrs) at rest.

Within the six-layer tissue model, the blood fraction was set to zero within the outermost layer, i.e., epidermis and dermis, which served as a wavelength-dependent attenuator. Fig.6 shows the contribution of the blood fraction to the three inner layers, i.e., papillary plexus, dermis, and cutaneous plexus. Specifically, the dermal layer contributes the most of the output signals and a stronger perfusion in the fingers is also revealed.

4. DISCUSSION

It has been shown that PPG signals after the exercise could be remotely accessed through an experimental OPI system. The performance of the OPI system has been evaluated by comparing it with a commercial pulse oximeter sensor. The strong correlation and good agreement between these two modes of detection suggest that the OPI system can successfully obtain data about cardiovascular variables such as heart rate and regional blood flow.

The optimal amount of exercise to maintain fitness and reduce mortality from cardiovascular disease remains a matter of debate. For instance, Lee and colleagues showed that moderate-intensity exercise training was sufficient to produce substantial benefits [16], while Williams argued that high-intensity training produced proportionally greater effects [17]. In the present study, two different exercise levels, which represent moderate- and high-intensity exercise respectively, were performed by 12 normotensive subjects. Compared to the resting condition, a gradual increase in SBP and HR was uncovered in the post-ex1and post-ex2 states, which agrees well with previous studies [18, 19]. Bland-Altman analysis showed that the physiological signals obtained from the OPI system compared well with the commercial contact-sensor, thus revealing the potential value of this remote technique in monitoring the pathophysiological response to the cardiovascular system to exercise as well as longer term monitoring of tissue perfusion in patients suffering from shock or injury.

Many previous PPG studies yield data only for a single site [1] and cannot provide information about skin perfusion and associated pulsatile processes. Driven by the demand for remote and reliable technology for clinical primary care and home health patient monitoring, imaging PPG has attracted much recent attention and has brought new insights into the characterization of vascular skin lesions [3-5, 20]. For example, a clear contrast in pulsatility between normal and adjacent port wine stain skin has been reported in [5], as has, a strong signal strength in areas of wounded skin when compared to healthy skin [3]. In the present study, it has been shown that a combination of Monte Carlo simulation and imaging PPG can provide a 3-D representation of blood perfusion in peripheral tissue and thus might lead to improved clinical assessment and diagnosis of circulatory pathology in various tissue segments.

A potential limitation of this work is the motion artifact. Since the sensor has no contact with the skin, movements of the subject relative to the camera can occur which might introduce artifact and lead to inaccurate results. Such a problem can, however, be solved by employing signal/image processing techniques for movement compensation and motion noise separation. Therefore, further investigation of imaging PPG signal with motion compensation/cancelation is needed. Another limitation is the quantification of the blood perfusion information. Since the main purpose of the present study is to propose and evaluate a novel OPI system, the perfusion was not fully investigated under different states. However, the quantified perfusion especially the contrast between normal and wounded skin provides valuable information. A future study with additional patient numbers and states will consider the performance of the blood perfusion mapping.

5. CONCLUSION

In this study, the novel OPI system coupling a sensitive CMOS camera and a customized RCLED ringlight was implemented to evaluate physiological changes during cycling exercise. The performance of the OPI system was analyzed with heart rate in 12 normotensive subjects. Compared to conventional contact pulse waveform measurements, the OPI system not only exhibits comparable functional characteristics in detecting pulsatile blood flow but also offers functional mapping of the blood perfusion status which could lead to new insights and applications in clinical assessment.

ACKNOWLEDGEMENTS

The authors are grateful to Loughborough University and Shanghai Jiao Tong University for their support, and TrueLight Corporation, who supplied the RCLEDs.

REFERENCES

[1] Allen, J., "Photoplethysmography and its application in clinical physiological measurement," *Physiol. Meas.*, 28, R1-39 (2007).
[2] Hertzman, A. and Spealman, C., "Observations on the finger volume pulse recorded photoelectrically," *Am. J. Physiol.*, 119, 334-335 (1937).
[3] Hulsbusch, M. and Blazek, V., "Contactless mapping of rhythmical phenomena in tissue perfusion using PPGI," *Proc. of SPIE*, 4683, 110-117 (2002).
[4] Wieringa, F. P., Mastik, F. and van der Steen, A. F. W., "Contactless multiple wavelength photoplethysmographic imaging: A first step toward 'SpO(2) camera' technology," *Ann. Biomed. Eng.*, 33, 1034-1041 (2005).
[5] Verkruysse, W., Svaasand, L. O. and Nelson, J. S., "Remote plethysmographic imaging using ambient light," *Opt. Express*, 16, 21434-21445 (2008).
[6] Farrell, S. W., KampertJ. B., Kohl, H. W., Barlow, C. E., Macera, C. A., Paffenbarger, R. S., Gibbons, L. W. and Blair, S. N., "Influences of cardiorespiratory fitness levels and other predictors on cardiovascular disease mortality in men," *Med. Sci. Sports Exerc.*, 30, 899-905 (1998).
[7] Quigley, F., "A survey of the causes of sudden death in sport in the Republic of Ireland," *Br. J. Sports Med.*, 34, 258-261 (2000).
[8] Iwasaki, K., Zhang, R., Zuckerman, J. H. and Levine, B. D., "Dose-response relationship of the cardiovascular adaptation to endurance training in healthy adults: how much training for what benefit?," *J. Appl. Physiol.*, 95, 1575-1583 (2003).
[9] Yoshiya, I., Shimada, Y. and Tanaka, K., "Spectrophotometric monitoring of arterial oxygen saturation in the fingertip," *Med. Biol. Eng. Comput.*, 18, 27-32 (1980).
[10] Yao, J. and Warren, S., "A novel algorithm to separate motion artifacts from photoplethysmographic signals obtained with a reflectance pulse oximeter," *Proc. 26th IEEE EMBS*, 2153-2156 (2005).
[11] Hu, S., Zheng, J. and Azorin Peris, V., "A study of opto-physiological modeling to quantify tissue absorbance in imaging photoplethysmography," *Proc. 32nd IEEE EMBS*, 1, 5776-5779 (2010).
[12] Reuss, J. L.,"Multilayer modeling of reflectance pulse oximetry," *IEEE Trans. on Biomed. Eng.*, 52, 153-159 (2005).
[13] Cennini, G., Arguel, J., Aksit, K. and van Leest, A., "Heart rate monitoring via remote photoplethysmography with motion artifacts reduction," *Opt. Express*, 18, 4867-4875 (2010).

[14] Hlawatsch, F., and Boudreaux-Bartels, G. F., "Linear and quadratic time-frequency signal representations," *IEEE Signal Proc. Mag.*, 9, 21-67 (1992).
[15] Bland, J. M. and Altman, D. G., "Statistical methods for assessing agreement between two methods of clinical measurement," *Lancet*, 1, 307-310 (1986).
[16] Lee, I. M., Hsieh, C. C. and Paffenbarger, R. S., "Exercise Intensity and Longevity in Men - the Harvard Alumni Health Study," *JAMA-J. Am. Med. Assoc.*, 273, 1179-1184 (1995).
[17] Williams, P. T., "Relationships of heart disease risk factors to exercise quantity and intensity," *Arch. Intern. Med.*, 158, 237-245 (1998).
[18] Wang, L., Pickwell-MacPherson, E., Liang, Y. and Zhang, Y., "Noninvasive cardiac output estimation using a novel photoplethysmogram index," *Proc. 31st IEEE EMBS*, 1746-1749 (2009).
[19] Lauer, M. S., Okin, P. M., Larson, M. G., Evans, J. C. and Levy, D., "Impaired heart rate response to graded exercise. Prognostic implications of chronotropic incompetence in the Framingham Heart Study," *Circulation*, 93, 1520-1526 (1996).
[20] Poh, M. Z., McDuff, D. J., and Picard, R. W., "Non-contact, automated cardiac pulse measurements using video imaging and blind source separation," *Opt. Express*, 18, 10762-10774 (2010).